

Spatio-Temporal Study of Phytoplankton Groups from Inherent Optical Properties (Iops) in The Ivorian Marine Coastline from 2010 To 2020

BEUGRE K. Yves. B.¹, MOBIO A. Brice H.¹, KOUADIO M. Jeanne¹, KASSI A. Jean-Baptiste¹ and DJAGOUA E. M. Valere¹

¹Centre Universitaire de Recherche et d'Application en Télédétection (CURAT)

Université Félix Houphouët-Boigny

BP: 801 Abidjan 22,

Côte d'Ivoire

ABSTRACT

Today global warming affects all environments including coastal marine environments. Climate change also affects the development and proliferation of phytoplankton groups often leading to the massive production of phytoplankton groups in marine waters. It is with this in mind that the study on the determination of phytoplankton groups from optical properties in Ivorian marine waters was initiated. This study showed a great diversity of phytoplankton in the Ivorian marine domain during the years 2010 and 2020. The data used in these studies are geospatial data (remote sensing) of the optical properties of the oceans, in particular the IOPs (inherent optical properties). These are the fusion data from the various SeaWiFS, MODIS, MERIS, VIIRS sensors from 2010 to 2020 from the various OrbView 2, NOAA, ENVISAT and AQUA satellites, in particular the absorption coefficient data for dissolved and detrital matter at 443 nm (adg), phytoplankton absorption coefficient data at 443 nm (aph), and dissolved and detrital particulate backscatter coefficient data at 443 nm (bbp). For the processing of these data the pixel-oriented classification method was used for the identification of phytoplankton groups. The SeaDAS v 7.4 software, allowed to process and analyze the data and the Envi 5.3 software allowed to perform the data classification. The values of inherent optical properties (IOPs) were obtained as well as the spatial distribution of phytoplankton groups, thus allowing the production of maps of IOPs and the production of spatio-temporal distribution maps of cyanobacteria and diatoms.

Keywords: Cyanobacteria, Diatoms, Inherent optical properties, Ivorian marine domain, Remote Sensing, Phytoplankton.

1. INTRODUCTION

Côte d'Ivoire, a country in the Gulf of Guinea, is a narrowly wide region open to the Atlantic Ocean. Knowledge of the marine population and the study of biodiversity are therefore important issues for the conservation and prevention of coastal marine resources. The Ivorian marine domain possesses a large productive ecosystem and a great biological diversity, thus favoring the development of socio-economic activities and a great growth of the population around the coast. All marine species are influenced by physical and biological parameters, the variabilities of which govern their dynamism. The evolution of the pelagic ecosystem in this region is largely influenced by climatic variations and spatio-temporal variability of hydrodynamic phenomena[4]. The Ivorian marine ecosystem is also called an upwelling ecosystem, and is characterized by seasonal variation. This upwelling phenomenon influences the evolution of phytoplankton, which are the main food for several pelagic species. Nutrients transported to the surface by upwelling contribute to phytoplankton development. In fact, phytoplankton plays an important role in the global carbon cycle through the binding of inorganic carbon during photosynthesis. Monitoring spatial and temporal variations in the distribution of phytoplankton groups at the global level is of paramount importance [1]; [2]. Marine biology plays a major role in ocean biochemical cycles. In particular, the phytoplankton biological pump is involved in the regulation of the amount of carbon in the atmosphere and would be highly sensitive to future climate change ([5]; [7]; [8]). As the main primary producer, phytoplankton underpin aquatic ecosystems and are able to respond rapidly to environmental disturbances (nutrient inputs, temperature changes, salinity, turbidity, turbulence or stratification),

whether of natural or anthropogenic origin [27]. Quantitative and qualitative changes within phytoplankton communities have an impact on the entire food chain ([29]; [22]). Early detection of dense and nuisance algal blooms is possible using remote sensing of ocean color, so it is important to monitor and evaluate their compositions, biomasses and spatial-temporal variability, but this remains a delicate task. The distribution of phytoplankton is very heterogeneous and its dynamics are very rapid [22]. Around the world, phytoplankton blooms occur in waters, and their proliferation often causes negative impacts by becoming toxic [11]. A large number of human activities are carried out along global coasts (tourism, fisheries, aquaculture) and the proliferation of phytoplankton impacts on socio-economic activities and human health and some phytoplankton species have an impact on human health and the global economy [12]. Events of increased growth of toxic phytoplankton (or harmful algal blooms, HAB) are expected to be more frequent in a climate change scenario [9]. In the context of the proliferation of certain species such as Diatoms and Cyanobacteria, some authors have focused on the inherent optical properties, thus showing a detection potential using the fourth derivative of the absorption coefficient of phytoplankton ([19];[20];[28]). Several studies have been carried out worldwide on phytoplankton groups, in particular those of [1];[2] and [30]. However, these studies have not yet been carried out off the Ivorian coast, and Ivorian waters are vulnerable to the dangers caused by the proliferation of phytoplankton. To better understand the ocean phenomena contributing to the development and proliferation of phytoplankton species, the use of remote sensing is an essential tool. As part of this study, we are led to map phytoplankton groups from the inherent optical properties, and identify them from the data. To do so, the work will consist of:

- To produce spatio-temporal maps of the various phytoplankton groups in Ivorian marine waters derived from the inherent optical properties.
- To show their evolution in the Ivorian marine domain

2. MATERIALS AND METHODS

2.1 Presentation of the study area

With a surface area of 2,325 km², 7% of the surface area of Côte d'Ivoire, the Ivorian coastline is 566 km long (Figure 1). The coastal environment is characterised by a vast lagoon system and the Ivorian coastline is divided into three main sectors [14]:

- The western sector between Tabou, Sassandra and Fresco (230 km), oriented 70°N ;
- The central sector between Fresco and Abidjan (Port Bouet) (190 km), oriented 81°N ;
- The eastern sector between Abidjan (Port Bouet) and the border (100), oriented 101°N.

The interlocking bathymetric curves show the presence of two submarine transform faults: the Saint Paul fault in the west and the Romanche fault in the east. The Ivorian coastline is fed by rivers that flow from north to south. There are two types of rivers. The first is made up of the four main rivers (the Cavally, the Sassandra, the Bandama and the Comoé, with respectively 30,000, 75,000, 97,000 and 78,000 km²), which have their source in the savannah zone, the second is made up of the coastal rivers, which have a hydrological regime that is more closely linked to the seasons in the coastal zone[15]. The fusion data used for this work comes from SeaWiFS, MODIS, MERIS, VIIRS sensors from 2010 to 2020 of the various OrbView 2, NOAA, ENVISAT and AQUA satellites and is available on the website <http://esa-oceancolour-cci.org> and is of the ascii type. The use of global multi-sensor satellite data for research, allows the most complete and coherent time series possible of ocean phenomena and ocean modeling worldwide to be distinguished. These are absorption coefficient data for dissolved and detrital matter at 443 nm (adg) from 2010 to 2020, phytoplankton absorption coefficient data at 443 nm (aph) from 2010 to 2020, backscatter coefficient data for dissolved and detrital matter particles at 443 nm (bbp) from 2010 to 2020. The following software was used to carry out this work:

- SeaDAS for the extraction of data and the processing of satellite data from the various sensors;
- Ocean data view for salinity data extraction and statistical data;

- ENVI 5.3 of RSI® (Research System Incorporation): it is a processing software, of images par excellence, it was used for most of the operations of processing the acquired fusion satellite images and the realization of the classification of the results obtained.

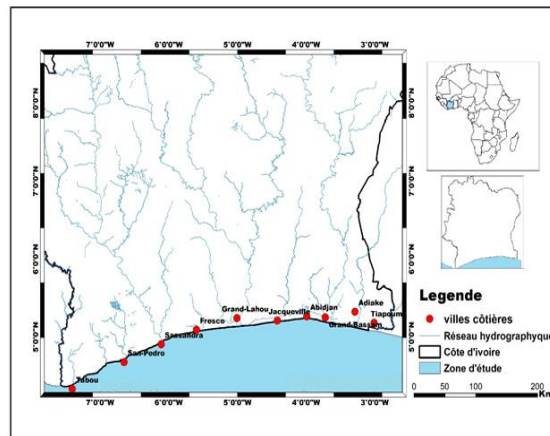


Figure 1. Map of the Ivorian marine coastline

2.2 Study Methodology

2.2.1 Analysis of Ocean Inherent Optical Properties

IOP data can be determined from different semi-analytical methods that apply to different types of water (case 1 and case 2). Absorption coefficient data for dissolved and detritic materials (a_{dg}), phytoplankton absorption coefficient (a_{ph}) and particle backscatter coefficient for dissolved and detritic materials (b_{bp}) were taken at wavelengths of 443 nm. The 443 nm band was chosen as it is a wavelength by which a_{cdom} and chlorophyll concentrations could be calculated. This is because it corresponds approximately to the mid-point of the peak photosynthetic action of most classes of algae in the blue spectrum.

2.2.2 Quasi-Analytical Algorithm (QAA)

This data was extracted with a version 5 of the multi-band Quasi Analytic (QAA) algorithm developed by [13] incorporated in the Seadas 7.5.3 software. The formulation proposed by [21] (equation) specifically emphasizes the effect of phytoplankton (a_{ph}) uptake, backscatter coefficient (b_{bp}) particles, and dissolved colored organic matter (a_{cdom}). For a given wavelength, the phytoplankton absorption coefficient, $a_{phy}(\lambda)$, is modeled according to Chl a as follows equation 1:

$$a_{phy}(\lambda) = A[\text{Chl } a]^{[E]} \quad (1)$$

$A(\lambda)$ and $E(\lambda)$ are the coefficients calculated by [6] from a large set of in situ measurements collected in oligotrophic, mesotrophic and eutrophic oceans.

Absorption by the dissolved organic matter is described in equation 2 below:

$$a_{cdom}(\lambda) = 0,065[\text{Chl } a]^{0,75} \exp(-0,014(\lambda - 443)) \quad (2)$$

Particle scattering and its spectral dependence are expressed according to relationships based on prior work. The particulate phase is constant and the variability of the b_{bp} coefficient particulate backscatter is directly related to that of b_p .

2.2.3 Validation of Inherent Optical Properties

Validation of inherent optical properties Unfortunately, the study of water color (reflectance) in relation to water constituents (IOPs) in Ivorian marine waters could not be conducted with in situ data. However, several validation studies, that of [18], have quantified the differences noted (ψ) between the MERIS values extracted from the QAA algorithm, noted x^M , and the in-situ measurements, x^f (MOBY station off Hawaii) of different oceans and covering a wide gradient of optical properties, from oligotrophic waters to waters rich in sediments or in CDOM as is the case of Côte d'Ivoire (equations 3, 4)

$$\psi = 100 \frac{1}{N} \sum_{i=0}^N \frac{x_i^M - x_i^f}{x_i^f} \quad (3)$$

$$rmsd = \sqrt{100 \frac{1}{N} \sum_{i=0}^N \left(\frac{x_i^M - x_i^f}{x_i^f} \right)^2} \quad (4)$$

Ψ is the mean difference between two distributions and $rmsd$ is the root-mean-square of the mean square of the values for estimating the uncertainties of the remotely detected reflectance (in sr^{-1}). A 10% and 14% bias was observed in wavelengths ranging from 490-560 nm, 16-18% in wavelengths of 443 nm, and 24-26% at 413 nm. The uncertainties on R_{RS} range from 0.0013 sr^{-1} to 413 nm and from 0.0002 sr^{-1} to 667 nm. These values are similar or lower than those obtained for MODIS-Aqua and SeaWiFS. Validation products between QAA products, in situ reflectance measurements, and IOPs revealed uncertainties of $0.17 \cdot 10^{-3}$ (sr^{-1}) for the total absorption coefficient a_t at wavelengths of 412, 443, and 490 nm, $0.31 \cdot 10^{-3}$ (sr^{-1}) for a_{ph} , and $0.22 \cdot 10^{-3}$ (sr^{-1}) for a_{CDM} [18]. Siegel studies [21]; [25] and [26] show global analyzes of inherent optical properties of water from the semi-analytical model GSM01 [16]. Also Siegel [25] and [26], also finds a good correspondence between the available in situ values and the SeaWiFS data (2000-2005). 64.3% and 80% respectively for a_{CDM} and b_{bp} at 440 nm, while the IOPs extracted from QAA applied to the available NOMAD data correspond to 82% and 83% (RSMD=0.29 and 0.26) for these same parameters at 43 nm. These uncertainties relate to the limitations of the algorithms used and the need to improve atmospheric correction and parameter extraction processes. However, they confirm the usefulness of MERIS image processing using SeaDAS [17] and the reliability of the QAA model in IOP extraction.

2.2.4 Extraction of phytoplankton groups pixel

Pixel-oriented supervised classification is the method used in this paper for categorizing the pixels of phytoplankton groups. Indeed, the supervised classification groups the pixels of a set of data into classes based on a_{ph} , a_{dg} and b_{bp} data that we have defined. Training data can be: Polygons, points, MultiPoint's from vector layers or existing shape files. Point or polygon shape files are created interactively on a loaded image. The training data must be defined before the supervised classification can continue. Once defined, the selected classes will be mapped to the output. The supervised classification method used is the minimum distance because it uses the average vectors for each class and calculates the Euclidean distance between each unknown pixel and the average vector for each class. The pixels are then classified in the closest class. Thus, the data of the optical properties can be categorized by virtue of the pixel-oriented classification incorporated in the ENVI 5.3 software.

3. RESULTS AND DISCUSSION

3.1 Results

3.1.1 Identification of Phytoplankton Groups from IOPs

Figure 2 shows the spatial and temporal distribution of phytoplankton groups from the absorption coefficient for dissolved and detrital matter (a_{dg}) from 2010 to 2020 in the ivorian marine coastline. Several studies, including those of [3], have shown that high values of a_{dg} are associated with diatoms and low values with cyanobacteria and other types of phytoplankton. Our identification of phytoplankton groups was achieved through this study. Figure 2 shows a large presence of diatoms and eukaryotes in the long cold season and in the transition period (October). These

phytoplankton groups occupy the broad coastlines and along the coast from west to east of our study area. In the large warm season and the small warm season, a decrease in diatoms and nanoeukaryotes is observed in the Ivorian marine domain. Phytoplankton are then observed along the coastline near the continental shelf. Cyanobacteria and other phytoplankton species are abundant in warm seasons and less abundant in cold seasons. In warm seasons, these groups occupy almost the entire study area, while in cold seasons they are further from shore.

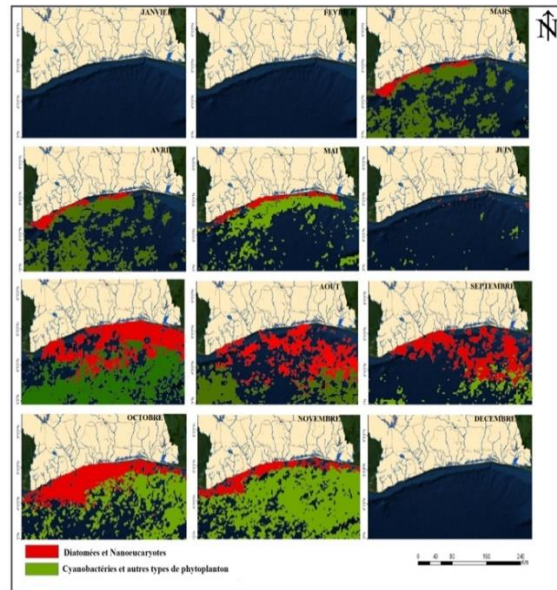


Figure 2. Spatial distribution of phytoplankton groups from the absorption coefficient (a_{dg}) from 2010 to 2020

Previous studies by [3] show that high a_{ph} values are associated with cyanobacteria and phytoplankton agglomerations. Figure 3 below shows the spatial distribution of a_{ph} values in the Ivorian marine coastline. This distribution tells us about the phytoplankton groups present in our study area from 2010 to 2020. During warm seasons, cyanobacteria occur along the coastline, near the continental shelf, and are less abundant. In the cold season (July and September) and in October, phytoplankton trees are observed near the coast and off the coast. This tree contains the cyanobacteria and phytoplankton agglomerations present in our study area. Diatoms and other phytoplankton groups are abundant in almost all seasons. For phytoplankton agglomerations, and other phytoplankton groups, our study could not be extended due to lack of in-situ data. Nevertheless, satellite imagery has enabled us to identify certain groups, including diatoms and cyanobacteria.

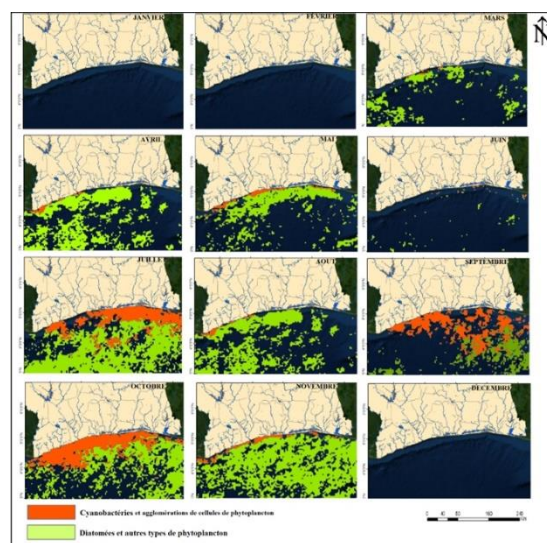


Figure 3. Spatial distribution of phytoplankton groups derived from the phytoplankton absorption coefficient (a_{ph}) from 2010 to 2020

Figure 4 illustrates the spatial distribution of the phytoplankton groups derived from the b_{bp} backscatter particles from 2010 to 2020. Overall spatial distribution analysis shows that diatoms and nanoeukaryotes are observed in cold seasons and near-shore October and are less abundant. These phytoplankton groups are virtually non-existent during warm seasons. They are represented in a narrow band near the continental shelf, along the coastline in our study area. Cyanobacteria and other phytoplankton groups occur in almost all seasons with dominance during warm seasons in our study area. High b_{bp} values and mean b_{bp} values are associated with diatoms and nanoeukaryotes, while low values are associated with cyanobacteria and other phytoplankton groups [3].

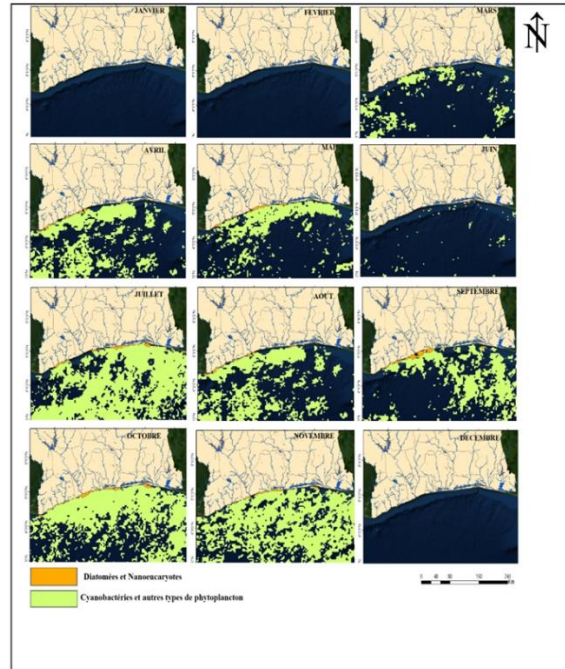


Figure 4. Spatial distribution of phytoplankton groups from the particle backscatter coefficient (b_{bp}) from 2010 to 2020

3.1.2 Evolution of phytoplankton groups from inherent optical properties

Figure 5 shows the evolution of phytoplankton groups from IOP's a_{dg} . The percentage of the pixel values of phytoplankton groups in the ivoirian marine domain is observed. Cyanobacteria and other unidentified phytoplankton groups reach peak percentages ranging from 12% to 28% depending on the different marine seasons. During the hot season they are 12% and during the cold season they are 28% more precisely in July. Low percentages of cyanobacteria and other unidentified phytoplankton groups are observed during the transition period in June. Generally mean values of cyanobacteria and other phytoplankton groups are also observed in almost all different marine seasons. High values of diatoms and nanoeukaryotes were observed during the high cold season in July (25%), while mean values were observed during the high and low hot seasons. Low values of diatoms and nanoeukaryotes are also observed in June. The percentages of phytoplankton groups derived from the present a_{dg} show an appearance and a nearly similar evolution of phytoplankton groups in the Ivorian marine domain.

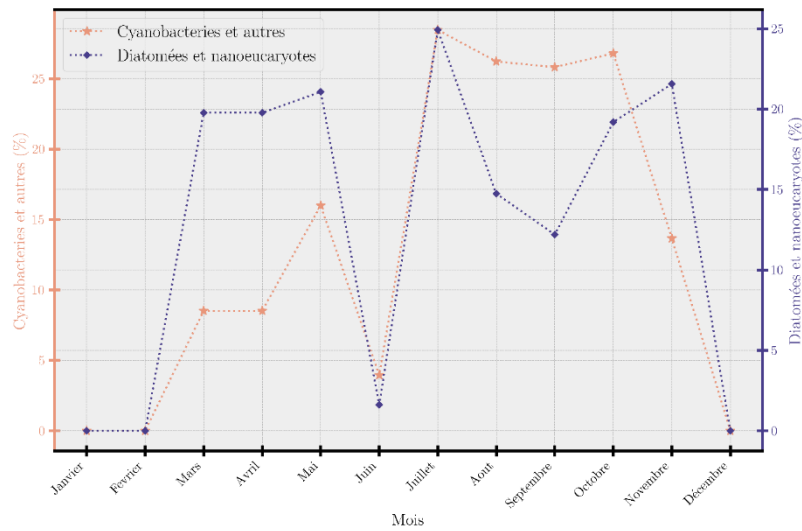


Figure 5. Variation of phytoplankton groups derived from a_{dg} from 2010 to 2020

Figure 6 shows the evolution of phytoplankton groups from the a_{ph} in the Ivorian marine domain. We observe that phytoplankton groups evolve almost identically during marine seasons on the Ivorian marine coast. Growth of cyanobacteria and others is observed during the hot summer season (15%) and October (30%), while diatoms and nanoeukaryotes have peaks between (25% and 30%) in July and November typical of cold marine seasons. The large hot season shows an average growth of phytoplankton groups. It is noted that June, December and the small cold season represent the lowest values of the phytoplankton groups.

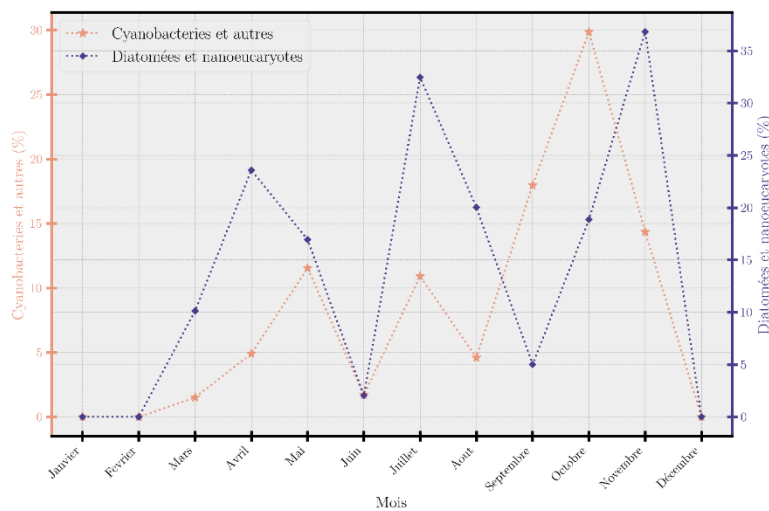


Figure 6. Variation of phytoplankton groups derived from a_{ph} from 2010 to 2020

Figure 7 shows the variation in phytoplankton groups from the b_{bp} backscatter coefficient from 2010 to 2020. The evolution of phytoplankton groups from b_{bp} is different from that of the a_{dg} (Figure 5), and of the a_{ph} (Figure 6), in the ivorian marine domain. Cyanobacteria and other phytoplankton groups have high values during the hot summer season and increasing values throughout the cold summer season, reaching a peak of 38% in October. As for diatoms and nanoeukaryotes, peak values are observed in the long cold season, in transition period (8%). Low phytoplankton group values are observed during the short cold season and the end of the short hot season.

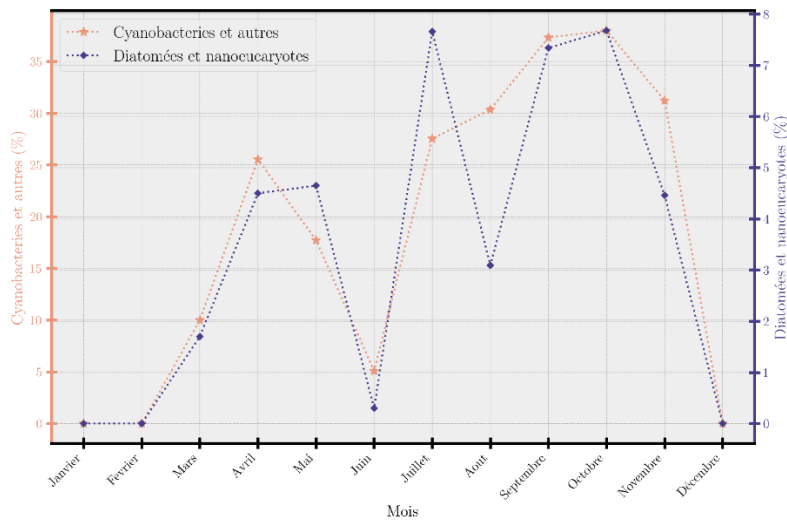


Figure 7. Variation of phytoplankton groups derived from b_{bp} from 2010 to 2020

3.1.3 Relationship between IOPs and phytoplankton groups

There is a relationship between the values of a_{dg} , a_{ph} and b_{bp} , and the occurrence of the different phytoplankton groups in the Ivorian marine domain (Table 1). Diatoms and nanoeukaryotes are identifiable in cold seasons and correspond to high and medium values of a_{dg} and b_{bp} . Cyanobacteria and other phytoplankton types are detectable in warm seasons and generally correspond to high a_{ph} values and low b_{bp} and a_{dg} values.

Table 1 : relationship between IOPs and phytoplankton groups

Seasons	a_{ph}	a_{dg}	b_{bp}	Phytoplankton groups
Great Season Cold	high / low	low / high	low / high	Cyanobacteria/other and Diatom/nanoeukaryotes
Great Season Warm	low / high	high / low	high / low	Cyanobacteria/other and Diatom/nanoeukaryotes
Small season Cold	None/None	None/None	None/None	None/None
Small season Warm	low / high	high / low	high / low	Cyanobacteria/other and Diatom/nanoeukaryotes
Period of Transition	high / low	low high	low / high	Cyanobacteria/other and Diatom/nanoeukaryotes

Legend: low (0.001 to 0.03 m^{-1}), high (0.03 to 1 m^{-1})

3.2 DISCUSSION

Data on the optical properties of the oceans, in particular those of the IOPs, have made it possible to demonstrate the spatio-temporal variability of the a_{dg} , b_{bp} and a_{ph} in Ivorian marine waters. The results provide information on the seasonal evolution of IOPs. Our results show that a_{dg} appear during the cold seasons and have an evolution almost similar to that of chlorophyll a, and that b_{bp} and a_{ph} evolve in the same way in the Ivorian marine domain. Our results are consistent with those of [10], which showed that changes in chlorophyll and sea surface temperature range from June to October, with a peak mainly in August-September coinciding with the coldest waters. Our results also showed

the presence of certain phytoplankton groups including diatoms, nanoeukaryotes and cyanobacteria in our waters. These groups are derived from the classification of the high, medium and low values of the optical properties IOPs. Each of these groups has its seasonal marine cycle off our coasts and are linked to the IOPs. The a_{dg} show that diatoms and nanoeukaryotes are related to high values of a_{dg} and occur during cold seasons. Cyanobacteria and other unidentified phytoplankton groups are related to low a_{dg} values and are abundant during warm seasons. Our results are consistent with those of [23] and [30], who showed that nanoeukaryotes are more abundant in cold periods than in hot periods. B_{bp} showed that diatoms and nanoeukaryotes were characterized by high values that were low, appeared more in the cold season and in periods of transition near the continental shelf, and cyanobacteria and other unidentified phytoplankton groups appeared more in the hot season. [3] showed that diatom-dominated waters are associated with higher values of b_{bp} and a_{dg} , and that b_{bp} values increase proportionally with cell diameter, which explains the relatively high values of spectral anomalies characterizing diatoms. On the other hand, diatom-dominated waters are characterized by the lowest a_{ph} values relative to the mean values. As for a_{ph} , high values are associated with cyanobacteria and low values with diatoms and nanoeukaryotes. In cold seasons our results show a medium proliferation of cyanobacteria and in hot seasons a proliferation of diatoms and nanoeukaryotes. Our results are in relation to those of [23] and [2] which showed that certain diatom species such as *Biddulphia sinensis* and *Hemiaulus membranaceus* appear in warm seasons. These results show that phytoplankton groups are found in a particular bio-optical environment.

4. GENERAL CONCLUSION

The main objective of the study in the Ivorian marine domain was to use geospatial data to detect phytoplankton types in order to contribute to better management of the Ivorian coastal marine environment. To achieve this objective, the study of ocean parameters such as inherent optical properties was carried out using satellite imagery. During the study period, the results also showed that certain optical properties have a different evolution of ocean parameters in the Ivorian marine domain. Our results also provide information on the spatial distributions of phytoplankton groups on our coasts. In the light of the results obtained, it emerges that remote sensing is an important tool for the characterization of phytoplankton groups in the Ivorian marine domain. A more detailed and regular study of the Ivorian marine domain by satellite imagery and marine sampling seems necessary to identify other toxic phytoplankton. Thus, it will be necessary to:

- Study phytoplankton groups by coupling in-situ data with satellite data;
- Perform laboratory measurements to understand optical processes

The study of all these parameters will make it possible to put in place a system to protect the state of health of the sea, in order to achieve management of the Ivorian coastal marine environment and fisheries management.

REFERENCES

- [1] ALVAIN S., MOULIN C., DANDONNEAU Y., et BREON F. M. (2005). Remote sensing of phytoplankton groups in case 1 waters from global SeaWiFS imagery. *Deep Sea Research I*, 52 : 1989-2004.
- [2] ALVAIN S., MOULIN C., DANDONNEAU Y., et LOISEL H. (2008). Seasonal distribution and succession of dominant phytoplankton groups in the global ocean: A satellite view. *Global Biogeochemical Cycles*, 22, GB3001, doi: 10.1029/2007GB003154.
- [3] ALVAIN S., LOISEL H., et DESSALLY D. (2012). Theoretical analysis of ocean color radiances anomalies and implications for phytoplankton groups detection in case 1 waters. *Optics Express*, 20, 1070-1083
- [4] ATILLA A., ORBI A., HILMI K. et MANGIN A. (2005). Produits opérationnels d'océanographie spatiale pour le suivi et l'analyse du phénomène d'upwelling marocain. *Géo. Observateur* n°14, p49-62.
- [5] BOPP L., MONFRAY P., AUMONT O., DUFRESNE L., TREUT H., MADEC G., TERRAY L., and ORR J. (2001). Potential impact of climate change on marine export production, *Global Biogeochem. Cycles*, 15(1).

- [6] BRICAUD A., BEDHOMME A-L ET MOREL A. (1988). Optical properties of diverse phytoplanktonic species; experimental results and theoretical interpretation. *Journal of Plankton Research*. vol. 10, no5, pp 851-873.
- [7] COX P., BETTS A., JONES C., SPALL S., and TOTTERDELL J. (2000). Acceleration of global warming due to carbon-cycle feedbacks in a coupled climate model, *Nature*, 408 P.
- [8] DUFRESNES J., FRIEDLINGSTEIN P., BERTHELOT M, BOPP L., CIAIS P., FAIRDHEAD L., LE TREUT H., and MONFRAY P. (2002). On the magnitude of positive feedback between future climate change and the carbon cycle, *Geophys. Res. Lett.*, 29(10), 1405, doi:10.1029/2001GL013777
- [9] GRIFFITH, A. W., AND GOBLER, C. J. (2020). Harmful algal blooms: A climate change co-stressor in marine and freshwater ecosystems. *Harmf. Algae* 91:101590. doi: 10.1016/j.hal.2019.03.008.
- [10] KOUADIO M.J. (2013). Suivi multi-temporel de la biomasse phytoplanktonique du littoral marin ivoirien : Apport de la télédétection à la détermination de l'origine et de la typologie des panaches chlorophylliens. Thèse Univ., Univ. de Cocody, p.1-146.
- [11] KLET J. (2013). Identification satellitaire des efflorescences de deux dinoflagellés, *Lepidodinium chlorophorum* et *Karenia mikimotoi*, grâce à leurs caractéristiques optiques. Université Bordeaux 1,p.1-28.
- [12] KUDELA, R. M., BERDELET, E., BERNARD, S., BURFORD, M., FERNAND, L., LU, S., ET AL. (2015), Harmful Algal Blooms. A Scientific Summary for Policy Makers. Paris: IOC/UNESCO, (IOC/INF-1320).
- [13] LEE Z.P., CARDER K.L AND AMONE R.A. (2002). Deriving inherent optical properties from waters color: A multi-band quasi-analytical algorithm for optically deep waters, *applied Optics*, vol.41, pp.5755-5772.
- [14] LEMASSON L., ET REBERT J-P. (1973). Courants marins dans le golfe ivoirien. *Cah. ORSTOM, Sér. Océanogr.*, vol. XI, n°1, pp.67-95.
- [15] LE LOEUFF P., ET MARCHAL E. (1993). Géographie littorale. In : *Environnement et ressources aquatiques en Côte D'Ivoire. I-Le milieu marin*. Paris, ORSTOM, p.15-22.
- [16] MARITORENA S., SIEGEL D.A AND PETERSON A. (2002). Optimization of a semi-analytical ocean color model for global scale applications, *Appl. Opt.*, vol. 41, pp.2705- 2714.
- [17] MELIN F. (2011b). Comparison of SeaWiFS and MODIS time series of inherent optical properties for Adriatic Sea. *Ocean Science*, vol.7, pp.351-361.
- [18] MELIN F., ZIBORDI G., BERTHON J-F, BAILEY SEAN, BRYAN F., VOSS K., FLORA S. AND GRANT M. (2011a). Assessment of MERIS reflectance data as processed with SeaDAS over the European seas. *Optically society of America*, vol. 19, n° 25, pp.25657- 25671
- [19] MILLIE, D. F., SCHOFIELD, O. M., KIRKPATRICK, G. J., JOHNSEN, G., TESTER, P. A., AND VINYARD, B. T. (1997). Detection of harmful algal blooms using photopigments and absorption signatures: a case study of the florida red tide dinoflagellate, *gymnodinium breve*. *Limnol. Oceanogr.* 42(5 Part 2), 1240–1251. doi: 10.4319/lo.1997.42.5_part_2.1240.
- [20] MILLIE, F, D., KIRKPATRICK, J, G., VINYARD, AND T, B. (1995). Relating photosynthetic pigments and in vivo optical density spectra to irradiance for the florida red-tide dinoflagellate *gymnodinium breve*. *Mar. Ecol. Prog. Ser.* 120, 65–75. doi: 10.3354/meps120065.
- [21] MOBLEY C.D., STRAMSKI D. (1993). oceanic waters. *Journal of Marine Research*, vol. 48, pp.145-175.
- [22] THYSSEN M. (2008). Analyse à haute fréquence spatiale et temporelle du phytoplancton à l'aide de la cytométrie en flux automatisée et immergeable. Thèse de doctorat. pp.217.
- [23] SEVRIN-REYSSAC J. (1993). Phytoplancton et production primaire dans les eaux marines ivoiriennes. In : *Environnement et Ressources Aquatiques de la Côte d'Ivoire. I-Le milieu marin*. Paris, ORSTOM, p.151-166.
- [24] SIEGEL, D. A., T. D. DICKEY, L. WASHBURN, M. K. HAMILTON, AND B. G. MITCHELL. (1989). Optical determination of particulate abundance and production variations in the oligotrophic ocean. *Deep-Sea Res. I* 36: 211-222.doi: 10.1016/0198-0149(89)90134-9.

- [25] SIEGEL D.A., MARITORENA S., NELSON N.B., HANSELL D.A. AND LORENZIKAYSER M. (2002b), Global distribution and dynamics of colored dissolved and detrital organic materials, *J. Geophys. Res.*, vol. 107, no C12, 3228, doi:10.1029/2001JC000965.
- [26] SIEGEL H., STOTTMEISTER I., REIMANN J., GERTH M., JOSE C. AND SAMIAJI J. (2009). Siak River System – East-Sumatra: Characterisation of sources, estuarine processes, and discharge into the Malacca Strait. *Journal of Marine Systems*, vol. 77, no 1-2, pp.148-159.
- [27] SMAYDA T.J. (1998) Patterns of variability characterizing marine phytoplankton, with examples from Narragansett Bay. *ICES Journal of Marine Science* Vol.55, Issue4, pp.562-573
- [28] STÆHR, P. A., AND CULLEN, J. J. (2003). Detection of *Karenia mikimotoi* by spectral absorption signatures. *J. Plankton Res.* 25, 1237–1249. doi: 10.1093/plankt/fbg083
- [29] STOCKNER J.G., ANTI N.J. (1986). Algal picoplankton from marine and freshwater ecosystems: A multidisciplinary perspective. *Can. J. Fish. Aquat. Sci.* 43: 2472-2503
- [30] ZIED B.M. (2013). Télédétection des groupes phytoplanctoniques via l'utilisation conjointe de mesures satellites, in situ et d'une méthode de classification automatique. *Océanographie. Université du Littoral Côte d'Opale*, p.1-33.